

Article

Model Based Generation Prediction of SPV Power Plant Due to Weather Stressed Soiling

Saheli Sengupta ¹, Aritra Ghosh ^{2,*} , Tapas K. Mallick ³ , Chandan Kumar Chanda ⁴, Hiranmay Saha ¹,
Indrajit Bose ⁵, Joydip Jana ¹ and Samarjit Sengupta ¹

¹ SAMGESS, IEST Shibpur, Howrah 711103, India; sahel.rs2021@cegess.iests.ac.in (S.S.); sahahiran@gmail.com (H.S.); joydipjana02@gmail.com (J.J.); samarsgp@gmail.com (S.S.)

² College of Engineering, Mathematics and Physical Sciences, Renewable Energy, University of Exeter, Cornwall TR10 9FE, UK

³ Environment and Sustainability Institute, Penryn Campus, University of Exeter, Penryn TR10 9FE, UK; T.K.Mallick@exeter.ac.uk

⁴ Electrical Engineering Department, IEST Shibpur, Howrah 711103, India; ckc_math@yahoo.com

⁵ Agni Power and Electronics Pvt. Ltd., Kolkata 700107, India; indrajitbose98@gmail.com

* Correspondence: a.ghosh@exeter.ac.uk

Abstract: Solar energy is going to be a major component of global energy generation. Loss due to dust deposition has raised a great concern to the investors in this field. Pre-estimation of this reduced generation and hence the economic loss will help the operators' readiness for efficient and enhanced economic energy management of the system. In an earlier article, a physics-based model is proposed for assessment of dust accumulation under various climatic conditions which is validated by data of a single location. In this paper, the universality of this model is established and is used to demonstrate the effect of generation loss due to dust deposition and of cleaning. Variation in the soiling pattern due to climatic covariates has also been studied. Generation loss is calculated for Solar Photovoltaic power plants of different capacities at various locations in India. Finally this model has also been extended to predict the generation accounting for the soiling loss in Photovoltaic system. All the calculated and predicted results are validated with the measured values of the above plants.

Keywords: dust accumulation; generation prediction; PV power; rebound; resuspension; soiling loss



Citation: Sengupta, S.; Ghosh, A.; Mallick, T.K.; Chanda, C.K.; Saha, H.; Bose, I.; Jana, J.; Sengupta, S. Model Based Generation Prediction of SPV Power Plant Due to Weather Stressed Soiling. *Energies* **2021**, *14*, 5305. <https://doi.org/10.3390/en14175305>

Academic Editor: Gabriele Grandi

Received: 27 July 2021

Accepted: 23 August 2021

Published: 26 August 2021

Publisher's Note: MDPI stays neutral with regard to jurisdictional claims in published maps and institutional affiliations.



Copyright: © 2021 by the authors. Licensee MDPI, Basel, Switzerland. This article is an open access article distributed under the terms and conditions of the Creative Commons Attribution (CC BY) license (<https://creativecommons.org/licenses/by/4.0/>).

1. Introduction

Although conventional energy resources contribute major component of global energy [1,2] their adverse effect toward environment by increasing carbon footprint, and green house gasses is of utmost concern. Moreover, global socio-political turmoil put an obstacle in importing and exporting these energy sources. Due to all these reasons, renewable energy generation has made its way towards the lion share of total generation, and it is expected that it becomes more than two-third of total generation by 2040 [3]. Considering the resource potential, SPV system is getting more priority. Trend shows that installed capacity of solar PV exceeded 500 GW at the end of 2018 and an additional 500 GW will be installed by 2022–2023 [4] which may be able to meet the expectation of global solar generation of 7200 TWh by 2040. PV power generation is largely correlated with the climatic conditions where it is installed [5–9]. Dust plays an important role in PV generation reduction predominantly in hot and humid climatic conditions. Generally, particulate matter with diameter less than 500 μm is called as dust [10]. It can be agricultural emissions, algae, bacteria, bird droppings, carpet, clay, engine exhaust, fibers, sand, textile, and pollen [11]. Deposited dust on a module reduces the transmittance of the module cover and hence allows less amount of sunlight to reach the solar cell which in turn abates the output rapidly [10].

Deposited dust on a PV system hugely depends on the properties of dust, PV tilt angle, surface material and local weather conditions. Thus, depending on the location,

PV power generation can be reduced from 5% to over 50%, if models are not cleaned [12]. Renewable integrated system has uncertainty due to stochasticity of sources which are mainly considered in economic system operation in [13,14]. However, most of the time, soiling loss is neglected in field operation. Reference [15] has reported that in 2018, 3–4% soiling loss caused EUR 3–5 Billion of revenue loss, which may increase to the extent of additional EUR 4–7 Billion by 2023. Cleaning of the module is only feasible if the PV system cleaning cost is less than the cost of the PV power loss due to dust [16]. The effect of different meteorological parameters on the dust deposition is investigated in [17]. Wind direction (WD) has good relationship with the module front surface, favorable wind direction causes the natural cleaning of module surface and reduces the module temperature [18]. Presence of relative humidity (RH) in atmosphere plays an important role in deposition velocity as water uptake by dust particle increases when hygroscopic material in dust is ~3.2% [19]. Increment of moisture in the atmosphere from 40% to 80% results increase of adhesion force by 80% [20,21]. Micheli et al. [22] shows a clear impact of intensity of rainfall on the soiling ratio (ratio between current output from soiled module and clean module). Limited rainfall causes more loss than dry weather condition whereas sufficient rainfall naturally cleans the module and increases the soiling ratio. The correlation between soiling rate and other climatic parameters are examined in [23]. Experimentation on soiling loss of PV modules of different technologies installed at the same location is carried out and presented in [24]. Seasonal variation causes the change in amount and chemical composition of airborne particle, which in turn alters the soiling rate [25,26]. An intensive review work made on the effect of dust on PV technology upto 2015 is explained in [27,28].

Dust deposition velocity is measured experimentally by Boyle et al. [29] and the results are compared with those obtained by Zhang et al. [30]. Classifying the limitations of this model, the authors asserted the need for a more descriptive model which will include all the soiling related parameters. B. Figgis et al. [19,31] has developed an “outdoor soiling microscope” to examine deposition phenomenon, and also made a field study on the effect of RH on deposition. Comparing the effects of dry and wet deposition and type of dust, it is found that wet deposition has higher negative impact than dry deposition [32]. Analysis of PV generation in a grid connected plant is made in most of the cases without considering the soiling loss or arbitrarily considering this loss [33–35]. Cumulative Damage Model has been used to study the effect of dust on long term PV power generation along with other environmental covariates [36]. Different simulation platforms are used to predict the amount of dust accumulation on a solar collector [37,38]. Mathematical representation of different relationships among dust and other meteorological parameters are discussed in [39]. A model is developed for estimating energy reduction due to dry deposition of dust from environmental data and orientation of module, and is validated with the field data [40]. The effect of RH and different types of precipitation in dust deposition are elaborated and validated with the field data [41].

From the literature survey, it is seen that a number of empirical models for calculation of soiling loss are proposed on the basis of laboratory experimental and field data. Subsequently a physics based model has also been proposed which is validated for a single location. This does not establish the efficacy of the model for PV plants with different capacities and locations. The novelty of this paper is to use this model extensively for plants of various capacities at different geographical locations in India. This is extended to propose a method for short term prediction of the PV generation which is validated by the measured data of a plant.

The objectives of this research are as follows: (a) show the utility of proper consideration of the soiling loss in generation calculation in field condition. Also the effect of dust accumulation on generation with and without cleaning is demonstrated. (b) Validation of the potential impact of PV power generation model embedded with wet and dry deposition concomitantly for different climates in India. (c) Evaluate and validate the power generation for range of different capacity power plants in India. (d) A short term prediction

for one month has been made and compared with the actual data for a plant in Gujarat, India.

The organisation of the paper is as follows: mathematical representation of the model is described in Section 2. PV plant details used for the calculation and validation of model are presented in Section 3, where the results are analyzed in Section 4. Finally, a conclusion is made in Section 5.

2. Methods

PV generation is dependent on various climatic parameters e.g., solar radiation, wind direction (WD), wind speed (WS), relative humidity (RH), precipitation and concentration of particulate material in the environment. As all these environmental covariates can be forecasted, the generation loss can also be predicted.

A model is formulated to develop fore-knowledge of reduced power $P_{plant_ac_pre}$ due to soiling using forecasted weather variables. In an ideal condition, module power output can be calculated by various ways; among them Anderson's model [42] is the most popular one. If a module has rated voltage and current V_{ref} and I_{ref} respectively, then with the incident radiation E (W/m^2), generated voltage and current can be calculated as,

$$v_{op} = V_{ref}(1 + a_v(T_{mod} - T_{aT})) \left(1 + a_E \left(\log \left(\frac{E}{E_{ref}} \right) \right) \right) \quad (1)$$

$$i_{op} = I_{ref}(1 + a_I(T_{mod} - T_{aT})) \left(\frac{E}{E_{ref}} \right) \quad (2)$$

However, in the field condition dust is accumulated on the module glass cover allowing less amount of radiation to reach the PV cell which reduces the output. This is accounted for as the transmission loss due to PV soiling and (1) and (2) can be modified as [40],

$$v_{op}' = V_{ref}(1 + a_v(T_{mod} - T_{aT})) \left(1 + a_E \left(\log \left(\frac{E * \Omega_r}{E_{ref}} \right) \right) \right) \quad (3)$$

$$i_{op}' = I_{ref}(1 + a_I(T_{mod} - T_{aT})) \left(\frac{E * \Omega_r}{E_{ref}} \right) \quad (4)$$

where, Ω_r is the reduced transmittance of the PV module, a_v , and a_I are the voltage and current temperature coefficients. This transmittance loss can be estimated by calculating the accumulated dust on the module surface as presented in (5), [43].

$$\Omega_r = \exp \left(- \frac{3 * \epsilon * m_{eff}}{8 \zeta_{PM} A_{PV} r_d \cos \theta_t \cos \Lambda} \right) \quad (5)$$

where, ϵ is the transmittance of a particle, Λ is angle of incidence (AOI).

Accumulated dust m_{eff} on the module is the remaining portion of the dust after rebound and resuspension of deposited dust. Particles can be deposited on the module by two processes e.g., dry and wet deposition. Dry deposition of dust is mainly due to eddy and molecular diffusion, gravitational settling, impaction and interception processes. Dust flux due to dry deposition on the surface is calculated as,

$$\Phi_d = -(e_d + D_d) \frac{d\zeta_{PM}}{dL} - \zeta_{PM}(V_t \cos \theta_t + V_{im}) \quad (6)$$

and the impaction velocity V_{im} is written [38] as (7)

$$V_{im} = \frac{\psi_i U_w \sigma_d}{1 + e^{-(\zeta_i(S_i - 1))}} \quad (7)$$

where, ψ_i is a weighting factor, ζ_t is a constant, S_t is the Stokes number and σ_d is a factor of the wind direction. Deposition flux can then be derived by integrating (6) and can be rewritten by incorporating wind friction velocity u_f^w as,

$$\int_{C_p}^0 \frac{u_f^w d\zeta_{PM}}{\Phi_d + \zeta_{PM}(V_t \cos \theta_t + V_{im})} + \delta_d \quad (8)$$

where,

$$\delta_d = \int_{\frac{L u_f^w}{\sigma_d}}^{\frac{r_d u_f^w}{\sigma_d}} \frac{dL^+}{\frac{e_d}{\sigma_d} + \frac{D_d}{\sigma_d}} \quad (9)$$

Solving (8) the amount of dust flux deposited on the module surface is obtained as (10).

$$\Phi_d = \frac{(V_t \cos \theta_t + V_{im}) \zeta_{PM} \exp \left[\frac{(-V_t \cos \theta_t - V_{im}) \cdot \delta_d}{u_f^w} \right]}{1 - \exp \left[\frac{(-V_t \cos \theta_t - V_{im}) \cdot \delta_d}{u_f^w} \right]} \quad (10)$$

Particle deposition with precipitation is represented by the term scavenging which is also called wet deposition or wet scavenging. Therefore, the scavenging rate (SR) [44] of particle is determined by (11)

$$S_R = \left[P_w^{-1/2} \left\{ \frac{0.24 + 0.64 R_e}{1 + R_e} \right\} + 4 \frac{r_d}{r_w} \left\{ \frac{1 + 2 V_w (r_d / r_w)}{1 + V_w R_e^{-1/2}} + \frac{r_d}{r_w} \right\} + \frac{S_t - S_t^{crit}}{S_t + \epsilon_t} \right] \cdot (p^r / 2D_m) \quad (11)$$

where, the first part of (11) is the collection efficiency due to molecular diffusion, P_w is Peclet number, ϵ_t is a constant and depends on the critical Stoke's number, and R_e is Reynolds number. Second part represents interception and the last term considers the effect of impaction. r_w is the radius of raindrop, V_w ratio of dynamic viscosity of water to air, S_t and S_t^{crit} are the Stoke's number and critical Stoke's number. From SR, the wet deposition flux can be calculated as,

$$\Phi_w = S_R p^r \zeta_{PM} \quad (12)$$

where, amount of precipitation p^r , D_m is volume-mean drop diameter. The mass of dust particle captured due to dry and wet deposition by the glass surface of the module during the time t is calculated as,

$$m_{dep}(t) = x_w \Phi_w A_{PV} t_r + x_d \Phi_d t_d A_{PV} \quad (13)$$

where,

$$x_w = \begin{cases} 0 & \text{if } p^r = 0 \\ 1 & \text{otherwise} \end{cases} \quad (14)$$

$$x_d = \begin{cases} 0 & \text{if } p^r \neq 0 \\ 1 & \text{otherwise} \end{cases}$$

and,

$$t_r + t_d = t \quad (15)$$

where, t_r is the time of rainfall and t_d is the time for dry deposition. It is considered in the model that at a particular time dust is deposited either by entirely precipitation (wet deposition) or by dry deposition in the presence of RH.

The total deposition due to dry and wet phenomena is represented in (13). After deposition on module surface, some portion of dust particles rebound immediately if the particles can overcome the particle-surface adhesion force. The velocity of the rebounded particle is determined by,

$$V_{re} = V_k \sqrt{\frac{e^2 (K_d^E + E_d) - E_{re}}{K_d^E}} \quad (16)$$

This rebound velocity V_{re} is used to determine the amount of rebounded mass $M_{rebound}$ of dust particle from the glass cover [39].

The particles on the tilted surface may also detach from its position due to external forces like wind force, gravitational force, or force due to rainfall (if there is any precipitation) by overcoming mainly the adhesion force. As capillary force dominates the adhesion force F_a in humid condition, increase of moisture content in the air reduces the resuspension rate of particles. Therefore, the resuspension rate is calculated [45] as (17),

$$\lambda_{res} = \zeta_o \exp \left[- \left(\frac{F_d}{F_\tau} \right)^\kappa \right] \quad (17)$$

where, κ and ζ_o are constants.

Drag force over the particle is as (16)

$$F_d = ((F_a + mg) \sin \theta_t + F_{ext} \cos \varphi_t) + F_r \cos \theta_t \quad (18)$$

and tangential pull-off force is written as (17),

$$F_\tau = \mu_w ((F_a + mg) \cos \theta_t + F_{ext} \sin \varphi_t) + F_r \sin \theta_t \quad (19)$$

where, the adhesion force F_a , it can be calculated as the sum of Van Der Waals force, capillary force and the force due to surface tension as given in (20).

$$F_a = \pi \gamma_S r_d \left[\frac{1}{\omega} \{ -\omega \cdot \sin \beta_c + \sin^2 \beta_c (\cos \theta_w + \cos \theta_{sw}) \} + \frac{1}{6 \gamma_S \pi h_c^2 X_v} \{ a_W (X_v - 1) - a_a \} + 2 \sin \beta_c \sin \theta_w \right] \quad (20)$$

where,

$$\omega = \frac{h_c}{r_d} + 1 - \cos \beta_c \quad (21)$$

$$\theta_w = (\beta_c + \theta_{pw}) \quad (22)$$

$$X_v = \frac{1}{[1 + r_d (1 - \cos \beta_c) / h_c]^2} \quad (23)$$

F_r is the force due to rainfall while light rainfall results in soiling but heavy rainfall promotes the natural cleaning phenomenon. F_r is obtained as [46,47] (24),

$$F_r = \frac{(1288.17 g_r^{-1.34} I_w^{1+1.34 \chi}) t_r}{\sqrt[3]{\frac{2 r_w^2 \rho_w g}{3 K_r}}} \quad (24)$$

where, χ and K_r are the constants, g_r is the value to describe the process of growth of raindrops, and I_w is the raindrop rate.

Now, the resultant accumulated mass of dust on the module surface after deposition, rebound and resuspension can now be written as (25),

$$m_{eff}(t) = \{ m_{dep}(t) - m_{reb}(t) \} \cdot \exp(-\lambda_{res} t) \quad (25)$$

If a plant is considered where N_p numbers of modules are connected in series in an array, then the generated voltage for that array will be

$$V_{op_s} = \sum_{i=1}^{N_p} v_{op}'(i) \quad (i = 1, 2, \dots) \quad (26)$$

The current output of the string with M_p number of arrays is determined as,

$$I_{op_s} = \sum_{j=1}^{M_p} i_{op}'(j) \quad (j = 1, 2, \dots)$$
(27)

The power output from each string can be determined as,

$$P_{dc} = V_{op_s} I_{op_s} FF$$
(28)

It is considered that the plant has P_i number of inverters with C_i number of channels in each inverter, then the total AC power output from the inverter is,

$$P_{plant_ac_pre} = \sum_{m=1}^{P_i} \left[\sum_{n=1}^{C_i} p_{dc}(C_i, P_i) \right] \varepsilon_{inv}(P_i)$$
(29)

The flow diagram for estimation of power generation using the model with different meteorological data is shown in Figure 1.

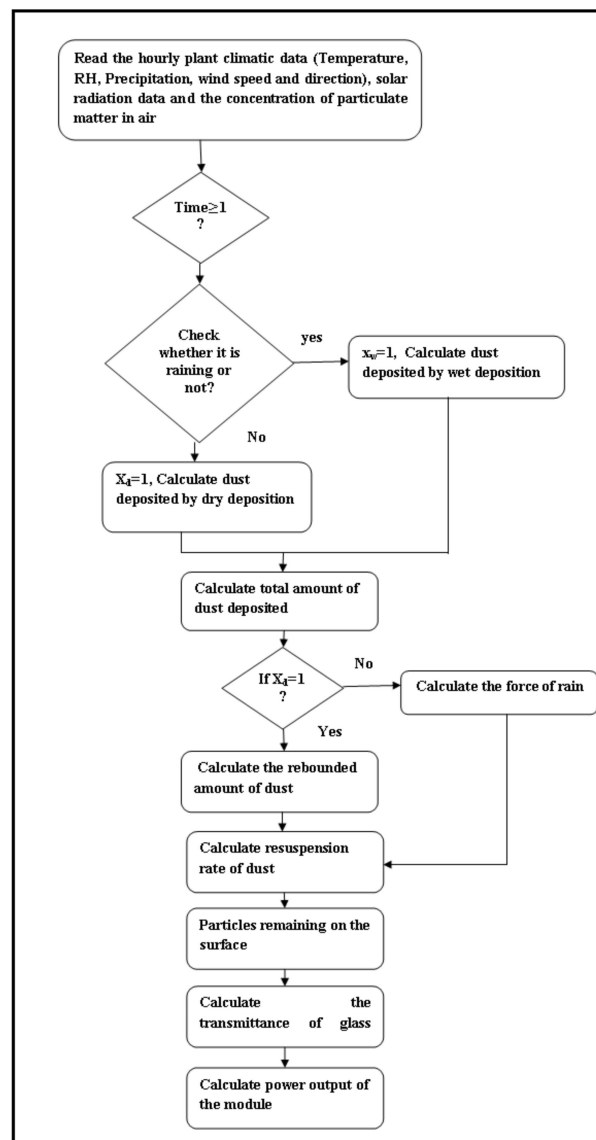


Figure 1. Flowchart of the model for soiling loss prediction.

3. PV Plant Details

Data for analysis are captured from four plants located at four different geographical locations of India. Particulate matter data of those locations are collected from the website of Central Pollution Control Board (CPCB), Government of India, and weather data are taken from a weather monitoring station [48]. Brief specifications of the four plants are as follows: (i) SPV power plant of Reserve Bank of India (RBI), Kolkata, capacity 50 kW_p, (ii) SPV power plant of Power Grid Corporation of India Ltd. (PGCIL), Nagpur, capacity 40 kW_p, (iii) SPV power plant of Hindustan Petroleum Corporation Ltd. (HPCL), Vishakhapatnam, capacity 100.8 kW_p, (iv) SPV power plant of NewTown Kolkata Development Authority (NKDA), Rajarhat, capacity 500 kW_p. The data available from the individual plants are used for the validation of the developed model. The details of the PV plants are given in the Table 1 and photographs of the plants are shown in Figure 2.

Table 1. Details of four SPV power plants.

Plant Name	Capacity	Location	Module Type	Inverter Type	Tilt Angle
PGCIL, Nagpur, Maharashtra	40 kW _p	21.14°N, 79.08° E	315 W _p , Multicrystalline	2 × RPI M20A (Delta)	20°
RBI, New Alipore, Kolkata	50 kW _p	22.57°N, 88.36° E	305 W _p , Multicrystalline	2 × RPI M10A 1 X RPI M30A (Delta)	20°
HPCL, Vishakhapatnam, Andhra Pradesh	100.8 kW _p	17.68° N, 83.19° E	315 W _p , Multicrystalline	5 × RPI M20A (Delta)	18°
NKDA, Rajarhat	500 kW _p	22.605691° N, 88.467579° E	295 W _p , Polycrystalline	25 × TRIO-20.0-TL-OUTD-400	7°



(a)



(b)



(c)

Figure 2. (a) HPCL, Visakhapatnam, Andhra Pradesh, (100.8 kW_p ground-mounted), (b) PGCIL, Nagpur, Maharashtra (40 kW_p roof-top), (c) NKDA, Rajarhat, Kolkata (500 kW_p canal top).

The meteorological data of the four plants at different locations in India during the period of validation of the model are shown in Figure 3. The values of RH, temperature, PM concentration, wind speed and solar irradiance of the four locations e.g., Andhra Pradesh, Maharashtra, Rajarhat and New Alipore are shown in Figure 3. The period of captured data for Rajarhat is January–February 2020, New Alipore is March–April 2021, whereas for the other two places this duration is January–February 2021. The data presented for all the four locations show that the PM concentration is and RH are sufficiently high. Irradiance seems to be better for Maharashtra than the other three locations, whereas the wind speed is more or less similar. Temperature for all the cases varies within the range of ~ 20 – 30 °C during the period considered.

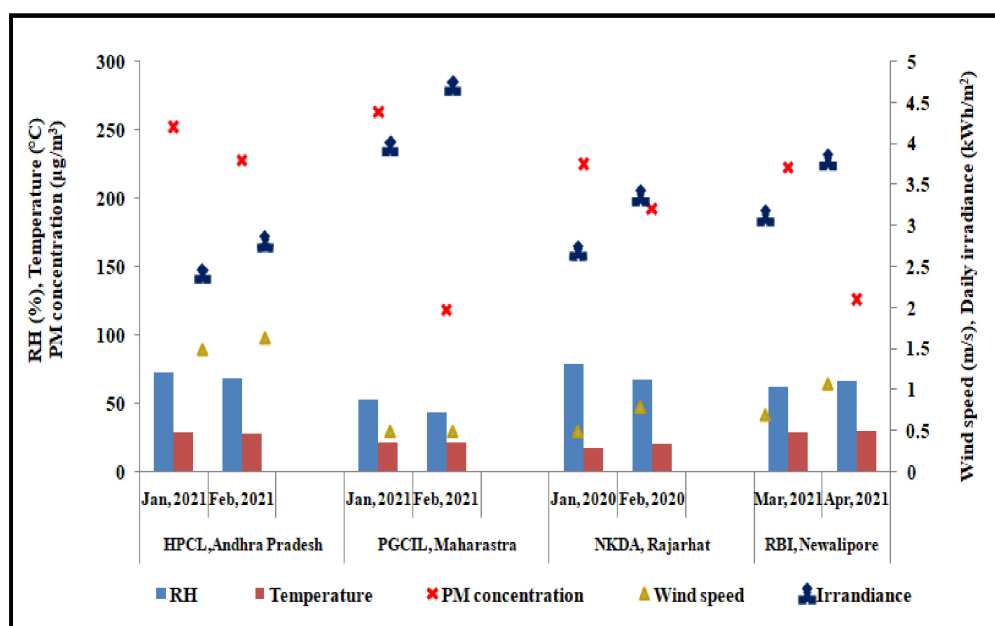


Figure 3. Climatic conditions for different location for the time period of calculation.

4. Results and Discussion

4.1. Validation of Model with and without Soiling Effect

Data captured from RBI, Kolkata are used to validate the model for with and without soiling effect of the PV modules. Figure 4 is the plant data which shows the radiation and power curves for 24 h with 5 min interval on 17 March 2021. From the figure it is clearly observed that the cleaning of modules is done between 1:12 pm and 1:47 pm so that the power output increases and maintains the higher generation. These two graphs indicate that at 10:15 am the generation is 15.25 kW with a radiation of 446 W/m² whereas at 13:48 pm (after completion of cleaning) the generation rises to 23.05 kW for 443 W/m² radiation.

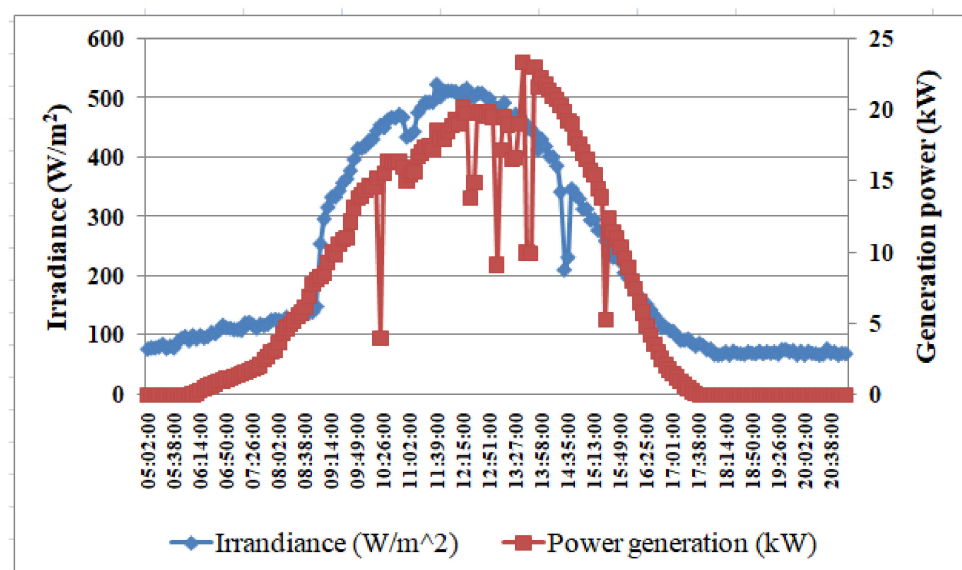


Figure 4. One day measured plant generation and radiation data on 17 March 2021 at RBI, Kolkata.

Figure 5 describes the comparison among measured energy, and calculated energy without and with dust from 1 March 2021 to 31 March 2021. Solar irradiance for this one month period is also overlapped in this figure. From Figure 6, it is seen that before the day of cleaning on 17 March 2021, difference between calculated energy without dust and measured one is higher whereas this reduces afterwards. The expected energy generation loss due to dust is 32.2% on 4 March 2021 for the irradiance 3.08 kWh/m^2 , whereas after cleaning this loss is only 8.15% on 26 March 2021 for almost the same radiation 3.07 kWh/m^2 .

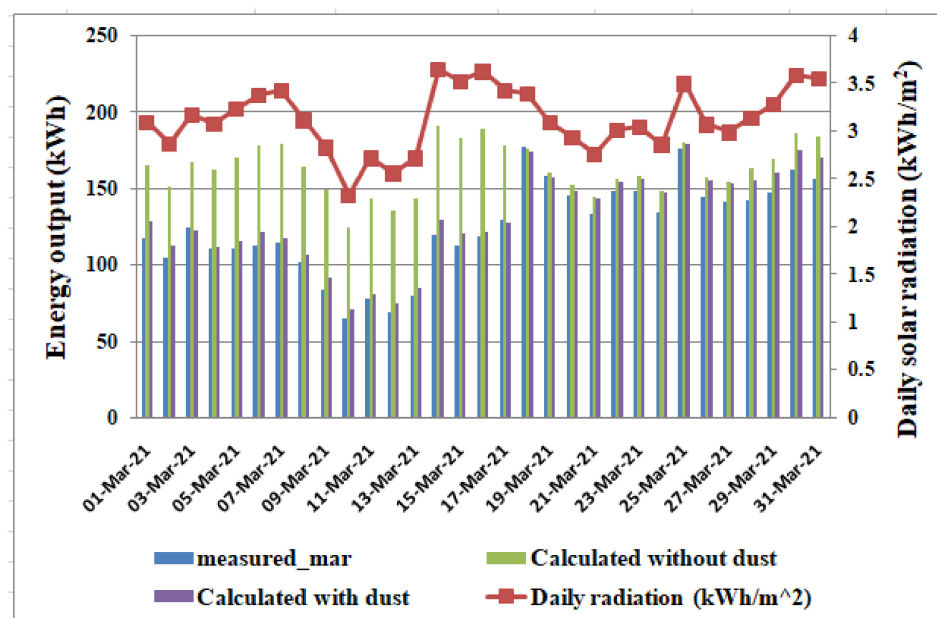


Figure 5. Comparison among measured plant generation, and model based calculated generation with and without dust from 1 March 2021 to 31 March 2021 at RBI, Kolkata (22.57° N , 88.36° E).

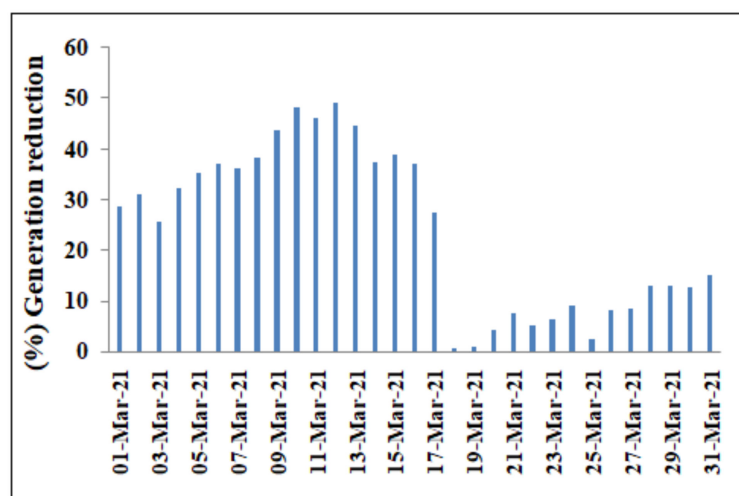


Figure 6. Calculated % Generation loss for one month at PV plant (RBI, Kolkata).

Loss due to soiling is analyzed based on one month data (from 1 March 2021 to 31 March 2021) of RBI, Kolkata, shown in Figure 7, under three specific conditions e.g., (a) model based calculated (%) soiling loss with cleaning, (b) calculated (%) soiling loss without cleaning, and (c) actual loss in field condition. Using the model it is observed that the soiling loss reduces from 43.3% (without any cleaning over the month) to 19.7% (with one time cleaning over same period as shown in Figure 4) whereas the field condition cumulative loss with one time cleaning comes out to be 23.7%. This exhibits the adverse effect of soiling on PV performance and the same time the advantage of cleaning.

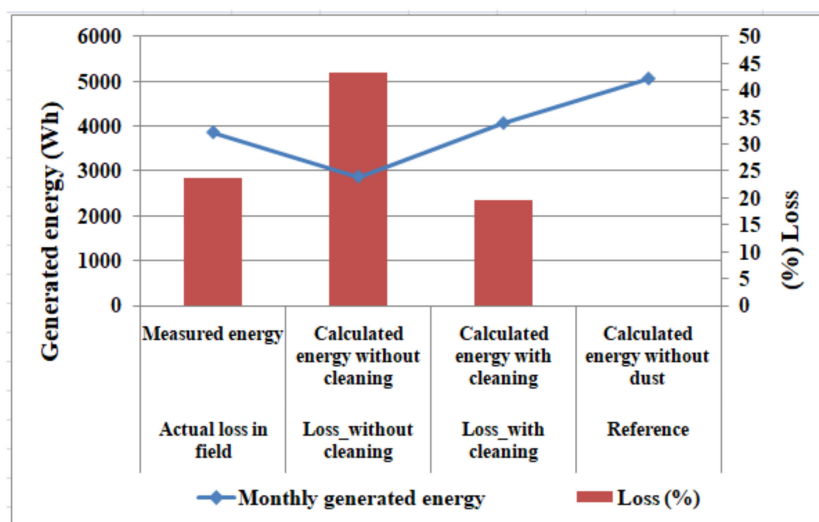


Figure 7. Analysis of soiling loss for one month.

4.2. Validation of the Model for Composite Climate Condition

The data of NKDA, Rajarhat, canal-top plant is used to validate the model for dust accumulation under composite weather conditions e.g., effects of no rain, drizzle, heavy rain, RH, and wind speed. From the Figure 8a,b, it is observed that on 2 January 2021 at 4 am (29th hour) at RH 93.26% (high), low wind speed 0.12 m/s and high PM concentration $302.44 \mu\text{g}/\text{m}^3$, and no rain causes cumulative dust accumulation of $35.53 \text{ mg}/\text{m}^2$ which is sufficiently high.

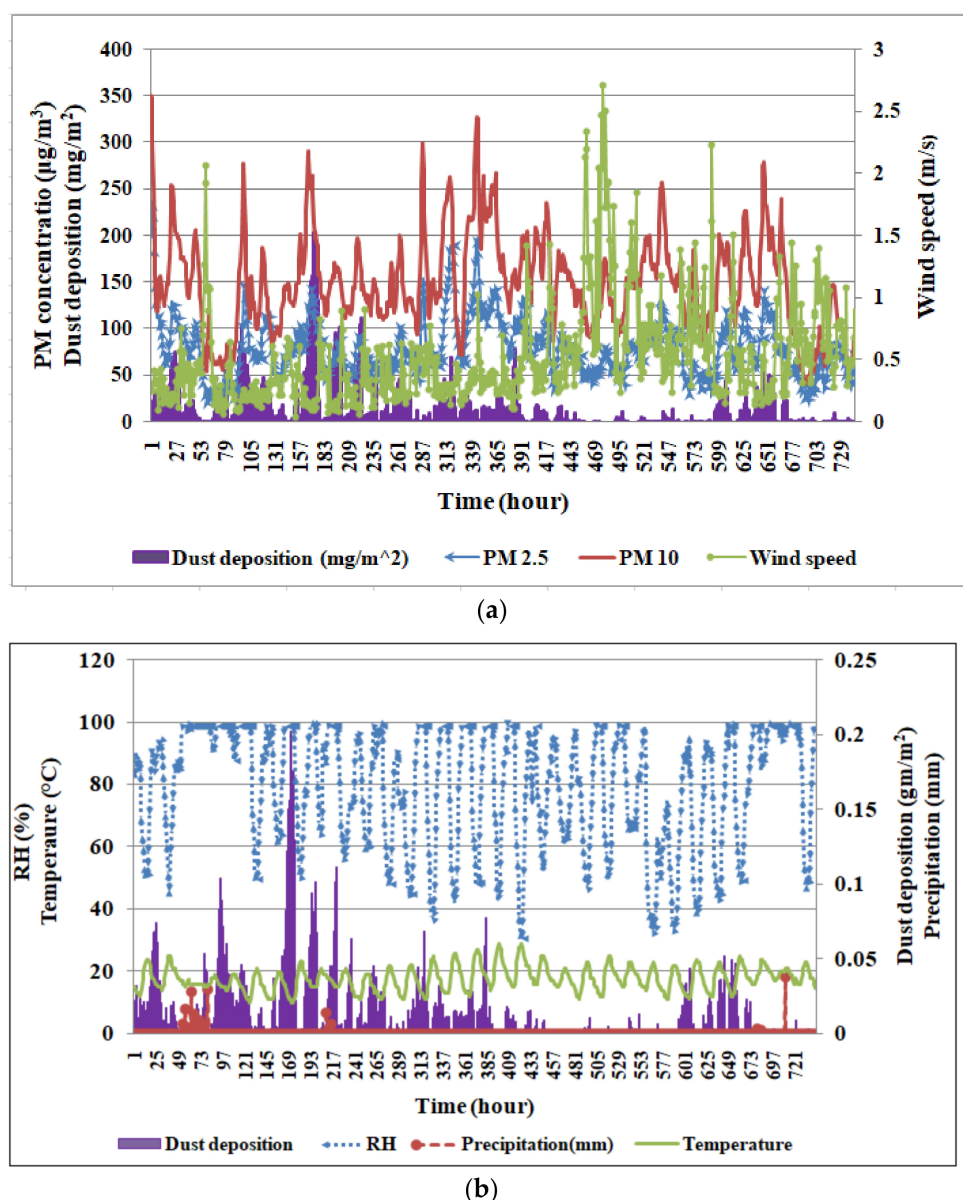


Figure 8. (a,b) Calculated deposited dust vis-à-vis the input weather data from 1 March 2021 to 31 March 2021.

At 81st hour (4 January 2021 8:00 am), with a low PM concentration of $128 \mu\text{g}/\text{m}^3$, heavy rainfall 13.94 mm, high RH 98.86% and wind speed 0.37 m/s, dust accumulation is negligibly small which indicates natural cleaning phenomenon.

With no rain, PM concentration $162.23 \mu\text{g}/\text{m}^3$, RH 94.18%, since the wind speed is moderately high, 2.19 m/s, the accumulation is negligibly small at 460th hour.

On 29 January 2021 at 10:00 am, it is observed that at no rain condition and PM concentration $147.55 \mu\text{g}/\text{m}^3$ the deposition is $0.42 \text{ mg}/\text{m}^2$ whereas in subsequent hour with almost similar other parameters but with a drizzle of 1.18 mm the deposition has doubled due to soiling effect.

From this qualitative analysis of Figure 8a,b, it is seen that the resultant accumulation corroborates with continuous change in the climatic parameters.

4.3. Validation of Model for Different Locations and Different Capacity

To validate the efficacy of the model, it is used to calculate the energy of three plants other than RBI, Kolkata, with different capacity located in different places in India. The

maximum daily error between measured and calculated energy considering soiling loss is within $\pm 10\%$ for all the cases. Figure 9 shows the model based energy generation with and without dust for these plants and makes comparison with the measure degeneration. The monthly soiling loss at field condition, calculated with respect to model based generation without dust (as obtained from the Figure 9), is obtained for HPCL plant 9% (January 2021), 6% (February 2021), PGCIL plant 6% (January 2021), 12% (February 2021), and NKDA plant 5% (January 2020), 7% (February 2020).

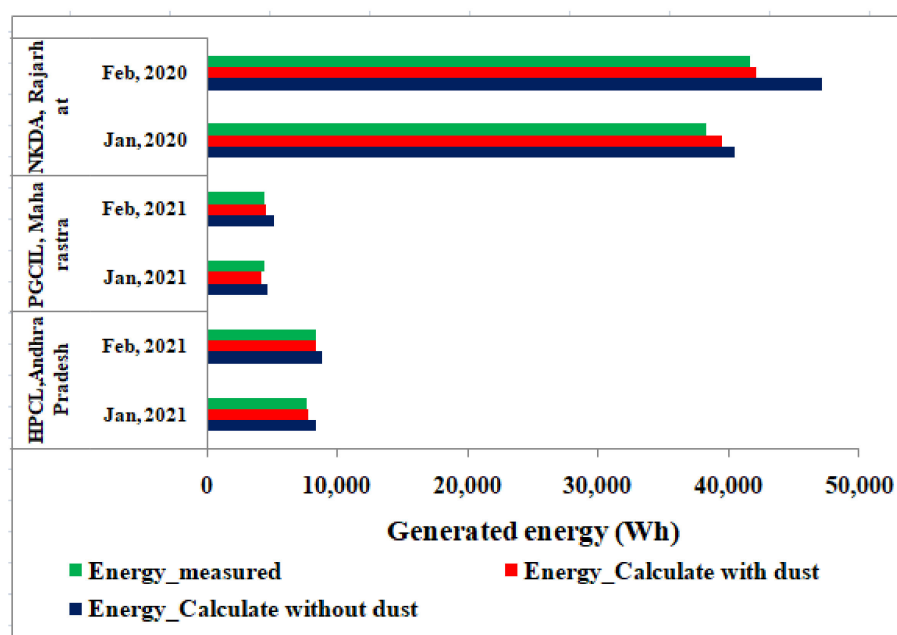


Figure 9. Validation of model for three different locations with different capacities in India.

4.4. Generation Prediction and Its Validation by Model

The model has been validated for PV generation and soiling loss assessment in the previous sections. In this subsection, this model is used for the prediction of PV generation and is compared with the measured value.

The generation prediction has been implemented with the data of a 3 MW_p PV plant in Gujarat, India. The plant has made up with mono-PERC PV module of capacity 395 W_p and 28 ABB inverters each 100 kW. Solar radiation data is taken from Solcast [49], pollution data is taken from the website of World's air quality index [50] and other parameters are taken from websites of CPCB and another weather monitoring station [48]. In Figure 10, portion 'ab' indicates the comparison between the actual generation and model based calculated generation for two months (from 1 April 2021 to 31 May 2021).

A comparison is made between the actual generation and predicted generation with forecasted weather data for one month (from 1 June 2021 to 30 June 2021) which is shown in portion 'bc'. The model based predicted generation for the month of June 2021 is obtained with the solar radiation data with 50% probability of occurrence. The generation scenario ranges from 10% probability of occurrence (lower profile of the shaded portion) to 90% probability of occurrence (upper profile of the shaded portion) of solar radiation along with other forecasted weather parameters. The actual generation exhibits a good match with the predicted one (portion 'bc') during the calculation period.

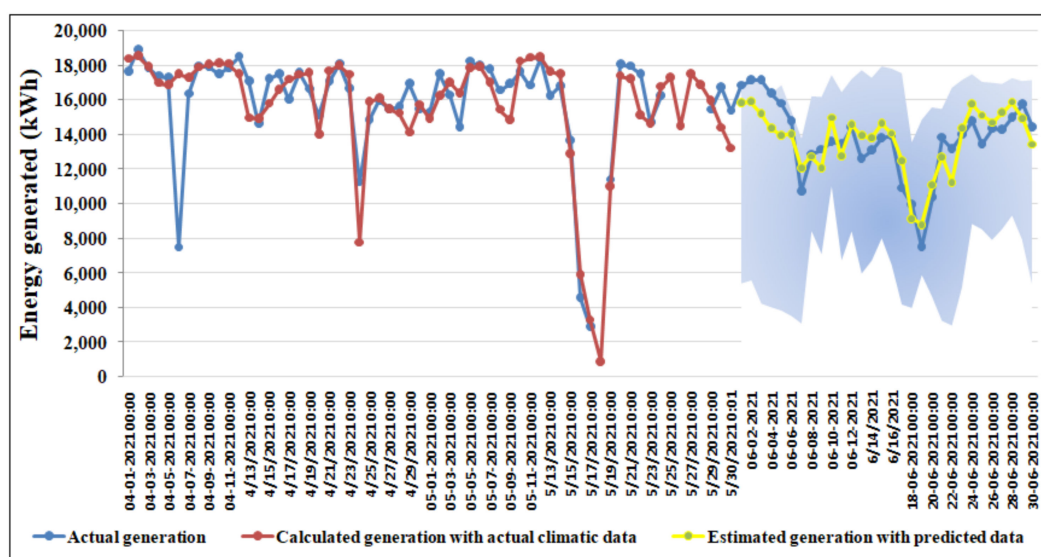


Figure 10. Model based PV generation prediction for 3 MW_P PV plant in Gujarat, India.

5. Conclusions

Soiling is an important parameter for PV integrated system as it invites yield loss which is reversible but not negligible. Pre-assessment of generation in field condition assures operators for economic and efficient energy management in a system. The contribution of this paper is that the physics-based model is used extensively to establish its universality for assessment of soiling loss of a PV power plant. It is validated step by step with the data captured from four plants of different locations and capacities in India. This has been extended for a short term prediction of power generation of a separate PV plant with the forecasted weather data and compared with the measured values.

The achievements of the paper are as follows:

- A model has been formulated for energy generation considering composite weather parameters and validated for four different SPV plants.
- The generation loss calculated from field data reaches upto ~50% (Figure 6) which is sufficiently high. For the same radiation $\sim 3.08 \text{ kWh/m}^2$, on 4 March 2021 the generation loss is 32.2% which comes down to 8.15% on 26 March 2021 after cleaning (Figures 5 and 6). This establishes the effect of cleaning.
- Validation of the model with and without soiling effects is carried out for RBI, Kolkata, SPV plant. Figure 7 demonstrates that the soiling loss is calculated as 43.3% for no cleaning over the month and 19.7% with one time cleaning for the same period. The field condition loss comes out to be 23.7% with one time cleaning. The model based assessment is well comparable with the field value.
- Expected dust accumulation variation with different climatic conditions e.g., effect of no rain, high wind speed, natural cleaning, soiling due to drizzling, all are established with the model based calculation for another plant at NKDA, Rajarhat, Kolkata for one month (Figure 8a,b).
- In the next step of validation, this model is used to calculate reduced generation for dust accumulation for three plants at different locations with different capacities (Figure 9) which shows monthly average loss for those plants ranges from 5–12%.
- Finally generation prediction is carried out for a 3 MW_P PV plant (Figure 10) and compared with the measured one showing a good match between them.

Usefulness of this research is three fold e.g., (i) short term prediction of generation loss will help the system operators' readiness for efficient operation, (ii) assessment of the loss will help in determining the optimum cleaning cycle for economic operation and (iii) a software can be developed with this model which may serve as an add-on tool with

existing PV system design software for calculation of effect of dust instead considering it arbitrarily.

Author Contributions: Conceptualization, methodology, validation, and formal analysis, S.S. (Saheli Sengupta) and A.G.; investigation, S.S. (Samarjit Sengupta) and J.J.; resources, J.J.; industrial data curation, I.B.; writing—original draft preparation, S.S. (Saheli Sengupta); writing—review and editing, A.G.; visualization, C.K.C.; supervision, T.K.M. and H.S.; project administration, funding acquisition, T.K.M. All authors have read and agreed to the published version of the manuscript.

Funding: This research was funded by RCUK’s Energy Programme, grant number EP/P003605/1.

Data Availability Statement: Not applicable.

Acknowledgments: The author Saheli Sengupta would like to acknowledge the fellowship support given by Department of Science and Technology (DST), Government of India (GoI) to carry out the research. The authors are also thankful to the University of Exeter, U.K for providing special glass coupons for the experimental work. PM concentration data is obtained from CPCB, GoI website, for which the authors are thankful. This work has been conducted as part of the research project ‘Joint UK-India Clean Energy Centre (JUICE)’ which is funded by the RCUK’s Energy Programme (contract no: EP/P003605/1). The projects funders were not directly involved in the writing of this article. In support of open access research, all underlying article materials (data, models) can be accessed upon request via email to the corresponding author.

Conflicts of Interest: The authors declare that there is no conflict of interest in the content of the paper.

Nomenclature

ed	Eddy diffusion coefficient
Dd	Molecular diffusion coefficient
aE	Radiation-temperature coefficient
T_{mod}	Module temperature
ζ_{PM}	PM concentration
V_t	Terminal velocity of the particle
V_k	Deposition velocity
θ_t	Panel tilt angle
F_{ext}	External force
U_w	Wind speed
θ_{sw}	Contact angle between surface and water in radian
ν_d	kinematic viscosity of air (m^2/s)
L	Height at which module is placed
CP	Particle concentration at the height L
rd	Particle diameter
μ_w	Coefficient of friction
E_{re}	Rebound energy
E_d	Deposition energy
β_c	filling angle
θ_{pw}	Contact angle between particle and water in radian
h_c	distance between particle and surface
a_W	Hamaker constant with water as medium
a_a	Hamaker constant with air as medium
APV	Area of photovoltaic module
γS	Surface tension energy
ϵ_{inv}	Efficiency of the inverter
E_{ref}	Reference radiation (1000 W/m^2)
T_a	Ambient temperature
ρ_w	Density of water
e	Coefficient of restitution
K_d^E	Kinetic energy of deposition
D_m	Mean-diameter of raindrop

References

1. Miller, B.G. Coal and energy security. *Clean Coal Eng. Technol.* **2011**, *1*, 585–612, ISBN 9781856177108.
2. Speight, J.G. Energy security and the environment. *Nat. Gas* **2019**, *2*, 361–390, ISBN 9780128095706.
3. IEA. *World Energy Outlook 2019*; IEA: Paris, France, 2019.
4. Haegel, N.M.; Atwater, H.; Barnes, T.; Breyer, C.; Burrell, A.; Chiang, Y.-M.; De Wolf, S.; Dimmler, B.; Feldman, D.; Glunz, S.; et al. Terawatt-scale photovoltaics: Transform global energy. *Science* **2019**, *364*, 836–838. [[CrossRef](#)] [[PubMed](#)]
5. Ghosh, A.; Sundaram, S.; Mallick, T.K. Colour properties and glazing factors evaluation of multicrystalline based semi-transparent Photovoltaic-vacuum glazing for BIPV application. *Renew. Energy* **2019**, *131*, 730–736. [[CrossRef](#)]
6. Alrashidi, H.; Issa, W.; Sellami, N.; Ghosh, A.; Mallick, T.K.; Sundaram, S. Performance assessment of cadmium telluride-based semi-transparent glazing for power saving in façade buildings. *Energy Build.* **2020**, *215*, 109585. [[CrossRef](#)]
7. Karthick, A.; KalidasaMurugavel, K.; Ghosh, A.; Sudhakar, K.; Ramanan, P. Investigation of a binary eutectic mixture of phase change material for building integrated photovoltaic (BIPV) system. *Sol. Energy Mater. Sol. Cells* **2020**, *207*, 110360. [[CrossRef](#)]
8. Karthick, A.; Ramanan, P.; Ghosh, A.; Stalin, B.; Kumar, R.V.; Baranilingesan, I. Performance enhancement of copper indium diselenide photovoltaic module using inorganic phase change material. *Asia-Pac. J. Chem. Eng.* **2020**, *15*, e2480. [[CrossRef](#)]
9. Alrashidi, H.; Ghosh, A.; Issa, W.; Sellami, N.; Mallick, T.K.; Sundaram, S. Thermal performance of semitransparent CdTe BIPV window at temperate climate. *Sol. Energy* **2020**, *195*, 536–543. [[CrossRef](#)]
10. Sarver, T.; Al-Qaraghuli, A.; Kazmerski, L.L. A comprehensive review of the impact of dust on the use of solar energy: History, investigations, results, literature, and mitigation approaches. *Renew. Sustain. Energy Rev.* **2013**, *22*, 698–733. [[CrossRef](#)]
11. Ghosh, A. Soiling Losses: A Barrier for India's Energy Security Dependency from Photovoltaic Power. *Challenges* **2020**, *11*, 9. [[CrossRef](#)]
12. Adinoyi, M.J.; Said, S.A.M. Effect of dust accumulation on the power outputs of solar photovoltaic modules. *Renew. Energy* **2013**, *60*, 633–636. [[CrossRef](#)]
13. Wei, J.; Zhang, Y.; Wang, J.; Cao, X.; Khana, M.A. Multi-period planning of multi-energy microgrid with multi-type uncertainties using chance constrained information gap decision method. *Appl. Energy* **2020**, *260*, 114188.
14. Wei, J.; Zhang, Y.; Wang, J.; Wu, L. Distribution LMP-Based Demand Management in Industrial Park via a Bi-Level Programming Approach. *IEEE Trans. Sustain. Energy* **2021**, *12*, 1695–1706.
15. Ilse, K.K.; Figgis, B.W.; Werner, M.; Naumann, V.; Hagendorf, C.; Pöhlmann, H.; Bagdahn, J. Comprehensive analysis of soiling and cementation processes on PV modules in Qatar. *Sol. Energy Mater. Sol. Cells* **2018**, *186*, 309–323. [[CrossRef](#)]
16. Ilse, K.; Micheli, L.; Figgis, B.W.; Lange, K.; Daßler, D.; Hanifi, H.; Wolfertstetter, F.; Naumann, V.; Hagendorf, C.; Gottschalg, R.; et al. Techno-Economic Assessment of Soiling Losses and Mitigation Strategies for Solar Power Generation. *Joule* **2019**, *3*, 2303–2321. [[CrossRef](#)]
17. Said, S.A.M. Effects of dust accumulation on performances of thermal and photovoltaic flat-plate collectors. *Appl. Energy* **1990**, *37*, 73–84.
18. Styszko, K.; Jaszczur, M.; Teneta, J.; Hassan, Q.; Burzyńska, P.; Marcinek, E.; Łopian, N.; Samek, L. An analysis of the dust deposition on solar photovoltaic modules. *Environ. Sci. Pollut. Res.* **2019**, *26*, 8393–8401. [[CrossRef](#)] [[PubMed](#)]
19. Figgis, B.W. Investigation of PV Soiling and Condensation in Desert Environments Via Outdoor Microscopy. Ph.D. Dissertation, ICube Lab., Uni. Strasbourg, Strasbourg, France, 2018.
20. Beattie, N.S.; Moir, R.S.; Chacko, C.; Buoni, G.; Roberts, S.H.; Pearsall, N.M. Understanding the effects of sand and dust accumulation on photovoltaic modules. *Renew. Energy* **2012**, *48*, 448–452. [[CrossRef](#)]
21. Mekhilef, S.; Saidur, R.; Kamalisarvestani, M. Effect of dust, humidity and air velocity on efficiency of photovoltaic cells. *Renew. Sustain. Energy Rev.* **2012**, *16*, 2920–2925. [[CrossRef](#)]
22. Micheli, L.; Muller, M. An investigation of the key parameters for predicting PV soiling losses. *Prog. Photovolt. Res. Appl.* **2017**, *25*, 291–307. [[CrossRef](#)]
23. Micheli, L.; Muller, M.; Kurtz, S. Determining the effects of environment and atmospheric parameters on PV field performance. In Proceedings of the 2016 IEEE 43rd Photovoltaic Specialists Conference (PVSC), Portland, OR, USA, 5–10 June 2016; pp. 1–6.
24. Micheli, L.; Caballero, J.A.; Fernandez, E.F.; Smestad, G.P.; Nofuentes, G.; Mallick, T.K.; Almonacid, F. Correlating photovoltaic soiling losses to waveband and single-value transmittance measurements. *Energy* **2019**, *180*, 376–386. [[CrossRef](#)]
25. Azarov, V.; Sergina, N.; Sidiyakin, P.; Kovtunov, I. Seasonal variations in the content of dust particles PM10 and PM 2.5 in the air of resort cities depending on intensity transport traffic and other conditions. *IOP Conf. Ser. Earth Environ. Sci.* **2017**, *90*, 1–10. [[CrossRef](#)]
26. Tanesab, J.; Parlevliet, D.; Whale, J.; Urmee, T. Seasonal effect of dust on the degradation of PV modules performance deployed in different climate areas. *Renew. Energy* **2017**, *111*, 105–115. [[CrossRef](#)]
27. Costa, S.C.S.; Sonia, A.; Diniz, A.C.; Kazmerski, L.L. Dust and soiling issues and impacts relating to solar energy systems: Literature review update for 2012–2015. *Renew. Sustain. Energy Rev.* **2016**, *63*, 33–61. [[CrossRef](#)]
28. Costa, S.C.S.; Diniz, A.S.A.C.; Kazmerski, L.L. Solar energy dust and soiling R and D progress: Literature review update for 2016. *Renew. Sustain. Energy Rev.* **2018**, *82*, 2504–2536. [[CrossRef](#)]
29. Boyle, L.; Flinchbaugh, H.; Hannigan, M. Assessment of PM dry deposition on solar energy harvesting systems: Measurement–model comparison. *Aerosol Sci. Technol.* **2016**, *50*, 380–391. [[CrossRef](#)]

30. Zhang, L.; Gong, S.; Padro, J.; Barrie, L. A size segregated particle dry deposition scheme for an atmospheric aerosol module. *Atmos. Environ.* **2001**, *35*, 549–560. [[CrossRef](#)]
31. Figgis, B.; Guo, B.; Javed, W.; Ahzi, S.; Rémond, Y. Dominant environmental parameters for dust deposition and resuspension in desert climates. *Aerosol Sci. Technol.* **2018**, *52*, 788–798. [[CrossRef](#)]
32. Chanchangi, Y.N.; Ghosh, A.; Sundaram, S.; Mallick, T.K. An analytical indoor experimental study on the effect of soiling on PV, focusing on dust properties and PV surface material. *Sol. Energy* **2020**, *203*, 46–68. [[CrossRef](#)]
33. Sharma, R.; Goel, S. Performance analysis of a 11.2 kWp roof top grid-connected PV system in Eastern India. *Energy Rep.* **2017**, *3*, 76–84. [[CrossRef](#)]
34. Kumar, B.S.; Sudhakar, K. Performance evaluation of 10 MW grid connected solar photovoltaic power plant in India. *Energy Rep.* **2015**, *1*, 184–192. [[CrossRef](#)]
35. Shukla, A.K.; Sudhakar, K.; Baredar, P. Simulation and performance analysis of 110 kW_p grid-connected photovoltaic system for residential building in India: A comparative analysis of various PV technology. *Energy Rep.* **2016**, *2*, 82–88. [[CrossRef](#)]
36. Sengupta, S.; Maiti, S.; Ghosh, S.; Das, A.; Sengupta, S.; Saha, H. A long term PV power degradation prediction due to dust fouling and environmental stresses. In Proceedings of the 2019 IEEE Region 10 Symposium (TENSYP), Kolkata, India, 7–9 June 2019; pp. 179–183.
37. Beegum, S.N.; Gherboudj, I.; Chaouch, N.; Couvidat, F.; Menut, L.; Ghedira, H. Simulating aerosols over Arabian eninsula with CHIMERE: Sensitivity to soil, surface parameters and anthropogenic emission inventories. *Atmos. Environ.* **2016**, *128*, 185–197. [[CrossRef](#)]
38. Liu, X.; Yue, S.; Lu, L.; Li, J. Study on dust deposition mechanics on solar mirrors in a solar power plant. *Energies* **2019**, *12*, 4550. [[CrossRef](#)]
39. Picotti, G.; Borghesani, P.; Cholette, M.E.; Manzolini, G. Soiling of solar collectors—modelling approaches for airborne dust and its interactions with surfaces. *Renew. Sustain. Energy Rev.* **2018**, *81*, 2343–2357. [[CrossRef](#)]
40. Sengupta, S.; Sengupta, S.; Saha, H. Comprehensive modeling of dust accumulation on PV modules through dry deposition processes. *IEEE J. Photovolt.* **2020**, *10*, 1148–1157. [[CrossRef](#)]
41. Sengupta, S.; Sengupta, S.; Chanda, C.K.; Saha, H. Modeling the Effect of Relative Humidity and Precipitation on Photovoltaic Dust Accumulation Processes. *IEEE J. Photovolt.* **2021**, *11*, 1069–1077. [[CrossRef](#)]
42. Anderson, A.J. *Photovoltaic Translation Equations: A New Approach*; Final Subcontract Rep. TP-411-20279; Nat. Renewable Energy Lab.: Golden, CO, USA, 1996.
43. Wang, J.; Gong, H.; Zou, Z. Modeling of Dust Deposition Affecting Transmittance of PV Modules. *J. Clean Energy Technol.* **2017**, *5*, 217–221. [[CrossRef](#)]
44. Slinn, W.G.N. Some approximations for the wet and dry removal of particles and gases from the atmosphere. *Water Air Soil Pollut.* **1977**, *7*, 513–543. [[CrossRef](#)]
45. Stempniewicz, M.M.; Komen, E.M.J.; de With, A. Model of particle resuspension in turbulent flows. *Nuclear Eng. Des.* **2008**, *238*, 2943–2959. [[CrossRef](#)]
46. Shin, S.S.; Park, S.D.; Choi, B.K. Universal Power Law for Relationship between Rainfall Kinetic Energy and Rainfall Intensity. *Adv. Meteorol.* **2016**, *2016*, 1–11. [[CrossRef](#)]
47. Zhou, G.; Wei, X.; Yan, J. Impacts of eucalyptus (*Eucalyptus exserta*) plantation on sediment yield in Guangdong Province, Southern Chin—a kinetic energy approach. *CATENA* **2002**, *49*, 231–251. [[CrossRef](#)]
48. Available online: <https://www.visualcrossing.com/weather/weather-data-services#/viewData> (accessed on 18 May 2020).
49. Available online: <https://solcast.com/> (accessed on 24 June 2020).
50. Available online: <https://waqi.info/> (accessed on 10 May 2021).